Lasers in Manufacturing Conference 2021

Development of laser-arc hybrid process for additive manufacturing of aluminum alloy and copper alloy

Dehua Liu[a], Shengnan Wu[a], Guangyi Ma[a, *], Fangyong Niu[a], Dongjiang Wu[a]

[a]*Key Laboratory for Precision and Non-traditional Machining Technology of Ministry of Education, Dalian University of Technology, Dalian, Liaoning Province 116024, PR China*

Abstract

Laser-arc hybrid process was recently suggested as a feasible method for additive manufacturing the metal structure with high properties and low defects. To promote an understanding of the effect of laser on manufacturing process, this paper is performed to prepare the Al-Zn-Mg-Cu alloy and Cu-Cr-Zr alloy using the laser and tungsten inert gas (TIG) arc hybrid heat source. The microstructure evolution of Al-Zn-Mg-Cu alloy and Cu-Cr-Zr alloy under laser-arc process are analyzed. Moreover, the elongation of the Cu-Cr-Zr alloy deposited sample can reach more than 40%. Laser-arc hybrid process provides a new idea for additive manufacturing alloys which are difficult to manufacture (high reflectivity, high thermal conductivity, et al.), and expand the application of laser additive manufacturing.

Keywords: Laser-arc hybrid; Additive manufacturing; High strength aluminum alloy; Copper alloy

1. Introduction

Al-Zn-Mg-Cu alloy has the advantages of high specific strength, low density, good corrosion resistance, while Cu-Cr-Zr alloy has high mechanical strength, excellent electrical and thermal conductivity, which make them widely used in the aerospace field [1-3]. As a fast and efficient near-net manufacturing method, laser additive manufacturing technology has high potential to produce complexity and large-scale structures [4].

Compared with titanium alloy and nickel base alloy, Al-Zn-Mg-Cu alloy has higher hot crack sensitivity [5], and Cu-Cr-Zr alloy has faster heat dissipation [6], which makes them difficult to form stable molten pool in the laser additive manufacturing. This problem restricts the development and further application for the additive manufacturing of Al-Zn-Mg-Cu alloy and Cu-Cr-Zr alloy. Stopyra et al. investigated the hot cracking

* Corresponding author.
E-mail address: gyma@dlut.edu.cn.

phenomenon of 7075 aluminum alloy during selective laser melting (SLM). They found that the density of deposited samples could reached 99%. However, the solidification crack could not be eliminated by process optimization [7]. Liu et al. prepared the C18400 copper alloy by SLM. The characteristics of high reflectivity and high thermal conductivity of copper alloy leads to less energy absorption in the SLM process, resulting in poor powder melting and low density [8]. In conclusion, it is necessary to carry out more innovative research to solve the problem of depositing for high reflection and high thermal conductivity alloys in laser additive manufacturing. Laser-arc hybrid additive manufacturing is suitable for alloys, like aluminum alloy or copper alloy. Because the arc with large heat input can melt the alloy to form molten pool, which increases the laser absorption rate. In addition, the laser-arc synergic effect can stabilize the additive manufacturing [9]. Liu et al. successfully fabricated 2219 aluminum alloy thin-walled samples without cracks by laser-arc hybrid method. They found that the grains in the laser zone were refined, and the degree of Cu element segregation was alleviated [10,11].

In this paper, the feasibility of preparing crack-free Al-Zn-Mg-Cu alloy and Cu-Cr-Zr alloy by laser-arc hybrid additive manufacturing is studied. The evolution of microstructure and the mechanical properties of the deposited samples are discussed.

2. Material and Experimental Procedures

The customized Al-Zn-Mg-Cu alloy and Cu-Cr-Zr alloy wires were used as feedstock. The chemical composition (wt.%) of Al-Zn-Mg-Cu alloy was 7.75 Zn, 1.43 Mg, 2.33 Cu, while the composition of Cu-Cr-Zr alloy was 0.95 Cr, 0.08 Zr. The deposited specimens were fabricated with the laser-arc hybrid additive manufacturing system shown in Fig. 1, which consisted of a Nd:YAG pulsed laser power, a TIG source, a wire feeder, and computer numerical control (CNC) platform. The argon gas was selected as shield gas with the flow rate of 15 L/min. Other process parameters are shown in Table 1.

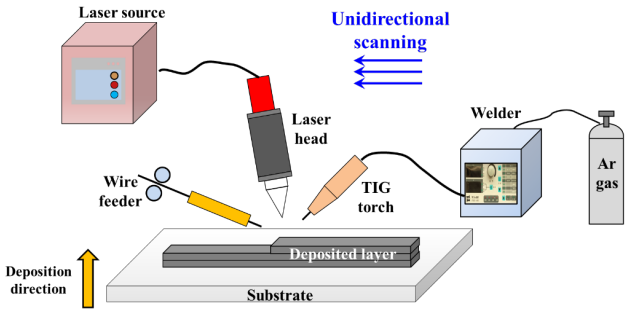

Fig. 1. Laser-arc hybrid additive manufacturing system

Table 1. Process parameters of the laser-arc hybrid additive manufacturing

	Al-Zn-Mg-Cu alloy	Cu-Cr-Zr alloy
Laser power (*W*)	200	100
Arc current (*A*)	120 A	170 A
Scan speed (*mm/min*)	250	200
Wire feeding speed (*mm/min*)	1500	1000

The metallographic samples were cut by electrical discharge cutting. Then, all samples were ground and polished to observe the microstructure and morphology. Optical microscopy (OM) analysis was used by OLYMPUS MX40F microscope. The microstructure and second phases were observed by ZEISS SUPARR 55 scanning electron microscope (SEM) with an energy dispersive X-ray spectrometer (EDS). The microhardness of the deposited sample was tested on the polished surface using a Vickers indenter (HUAYIN, DHVS-1000A) with 100 g load for 15 s. According to ISO 6892-1:2009 standard, the tensile specimen and tensile test method were designed. The tensile tests were performed at a tensile rate of 2 mm/min.

3. Results & Discussions

3.1. Macrostructure

Fig. 2 displays the surface morphologies of the single layer and multi-layers thin-walled samples of Al-Zn-Mg-Cu alloy prepared by laser-arc hybrid process. There is no crack defect inside the deposited samples along *XOZ* plane. The shape of the single layer is wide at the top and narrow at the bottom (Fig. 2b). The top region is mainly affected by arc, which is called arc zone (AZ). The bottom region is affected by laser, called laser zone (LZ). As shown in Fig. 2d, the periodic stripes are distributed on the *XOZ* plane of the multi-layers deposited sample, resulting in a periodic distribution of microstructure.

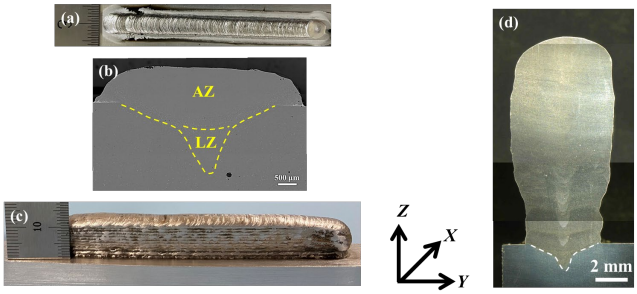

Fig. 2. Macrostructure morphology of the Al-Zn-Mg-Cu alloy deposited samples: (a) and (b) single layer; (c) and (d) multi-layers

3.2. Microstructure

As shown in Fig. 3a, the grains are seen clearly in the Al-Zn-Mg-Cu alloy deposited sample after polish and corrosion. The grain characteristics of each layer can be divided into columnar grains in the AZ and equiaxed grains in the LZ. The LZ is mainly affected by the laser energy, so the temperature gradient (*G*) is large.

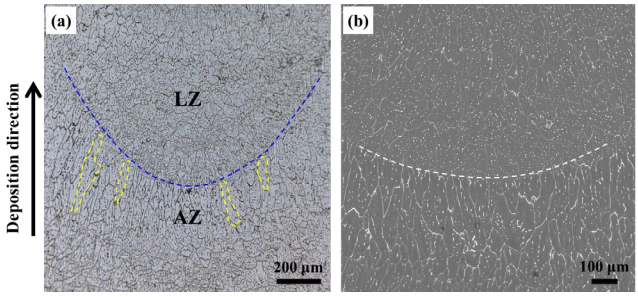

Fig. 3. (a) Grain morphology of the Al-Zn-Mg-Cu alloy deposited sample; (b) second phase characteristics

During the solidification process, it is beneficial to generate numerous grain nucleus and develop into equiaxed grains [12]. Under the combined action of arc and laser in the AZ, the cooling rate is slow, and the growing direction is closest to the thermal gradient in the molten pool, which is beneficial to the formation of columnar grains. Moreover, the white second phase in the LZ is uniformly distributed, while that in the AZ is coarse and enriched on the grain boundaries (Fig. 3b).

The microstructure of Cu-Cr-Zr alloy deposited sample is observed of the scanning direction (*XOY* plane), and the sample location is presented in Fig. 4a. Fig. 4c depicts the grain morphology at different positions along the *XOY* plane. The Cu-Cr-Zr alloy has good thermal conductivity and strong heat dissipation ability [13]. With the movement of the laser-arc hybrid heat source, the heat accumulation from the beginning to the end of the deposit process is not obvious, thus the grain size at different positions has no change. Fig. 4b and d present the grain morphology of the deposition direction (*XOZ* plane). The region near the substrate is columnar grain region. Due to the change of the heat dissipation and *G* at the top region, the columnar grains gradually transform to equiaxed grains.

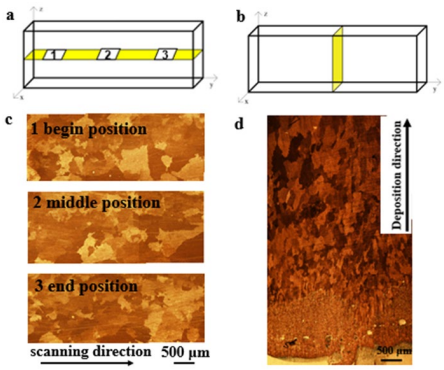

Fig. 4. (a) Sample position on the *XOY* plane; (b) microstructure on the *XOY* plane; (c) sample position on the *XOZ* plane; (d) microstructure on the *XOZ* plane

In Fig. 5, the chemical compositions of different phases in Al-Zn-Mg-Cu alloy were determined by EDS. The result shows that the position 1 is α-Al matrix, with Zn and Mg dissolved in it. The white structures (position 2) distributed on the grain boundaries. The elemental composition includes Al, Zn, Mg and Cu. This indicates they are eutectics, similar to the situation in wire + arc additive manufacturing of Al-Zn-Mg-Cu alloy [14].

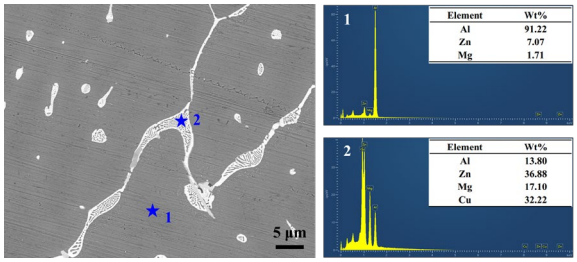

Fig. 5. Microstructure of the second phase and EDS spectrums of the Al-Zn-Mg-Cu deposited sample

Fig. 6 demonstrates the SEM microstructure of Cu-Cr-Zr alloy deposited sample under backscatter mode. Some round phases are distributed uniformly inside the grains. It can be concluded to be Cr-rich phase by EDS.

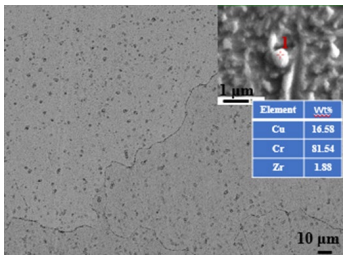

Fig. 6. Microstructure and EDS result of Cu-Cr-Zr alloy

3.3. Mechanical properties

The microhardness distribution of Al-Zn-Mg-Cu alloy along the deposition direction is shown in Fig. 7. The measurement distant between each point is 0.5 mm. The average microhardness of the deposited sample is 131.6 ± 12.2 $HV_{0.1}$. The microhardness values of the AZ and LZ are 131.3 $HV_{0.1}$ and 144.8 $HV_{0.1}$, respectively. The value of the LZ is approximately 10.3% higher than that of the AZ. Since the grain size in the LZ is much smaller than that in the AZ, its value is increased.

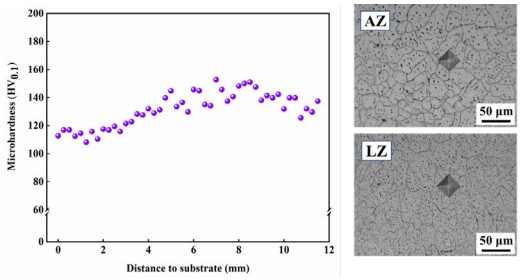

Fig. 7. Microhardness distribution of the Al-Zn-Mg-Cu alloy deposited sample

The three tensile specimens of Cu-Cr-Zr alloy are prepared along the scanning direction (Fig. 8a). The tensile test shows that the average tensile strength of the deposited samples is 233.4 ± 4 MPa, and the elongation is 41.3 ± 4.5%. Compared with the as cast sample [15,16], the tensile strength and elongation are increased by 14.2% and 37.7%, respectively. Fig. 8b illustrates the morphology of tensile fracture of the Cu-Cr-Zr alloy deposited sample. There are a number of dimples in the fracture. Thus, the fracture mode is ductile fracture.

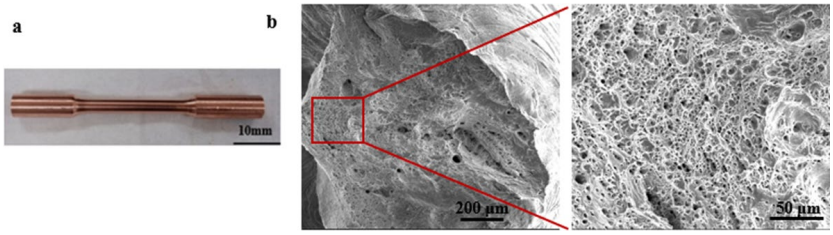

Fig. 8. (a) Tensile specimen of Cu-Cr-Zr alloy (b) morphology of tensile fracture

4. Conclusions

The microstructure and mechanical properties of Al-Zn-Mg-Cu and Cu-Cr-Zr alloys prepared by laser-arc hybrid additive manufacturing were investigated. There is no crack defect in the deposited samples. The grains in the LZ of the Al-Zn-Mg-Cu alloy are much smaller than that in the AZ, resulting in larger microhardness in the LZ. The columnar grains are distributed near the substrate and become equiaxed grains at the top of Cu-Cr-Zr alloy deposited sample. The tensile strength of the Cu-Cr-Zr alloy is 233.4 ± 4 MPa, and the elongation is 41.3 ± 4.5%. Moreover, the fracture mode is ductile fracture.

Acknowledgements

The authors would like to acknowledge the financial support from the National Natural Science Foundation of China (No. 51790172, 51805070).

References

[1] Fridlyander, I., Senatorova, O., 1996. Development and application of high-strength Al-Zn-Mg-Cu alloys, Materials Science Forum 217-222, p. 1813.

[2] Jha, K., Neogy, S., Kumar, S, Singh, R., Dey, G., 2021. Correlation between microstructure and mechanical properties in the age-hardenable Cu-Cr-Zr alloy, Journal of Nuclear Materials 546, 152775.

[3] Zhang, Z., Sun, L., Tao, N., 2020. Nanostructures and nanoprecipitates induce high strength and high electrical conductivity in a CuCrZr alloy, Journal of Materials Science and Technology 48, p. 18.

[4] Calignano, F., Manfredi, D., Ambrosio, E., Iuliano, L., Fino, P., 2013. Influence of process parameters on surface roughness of aluminum parts produced by DMLS, The International Journal of Advanced Manufacturing Technology 67, p. 2743.

[5] Qi, T., Zhu, H., Zhang, H., Yin, J., Ke, L., Zeng, X., 2017. Selective laser melting of Al7050 powder: Melting mode transition and comparison of the characteristics between the keyhole and conduction mode, Materials and Design 135, p. 257.

[6] Jiang, W., Yu, R., Lu, S., 2013. Effect of compound fluxes on A-TIG welding joint depth of Cu-Cr-Zr alloy, Materials Science Forum 749, p. 133.

[7] Stopyra, W., Gruber, K., Smolina, I., Kurzynowski, T., Kuźnicka, B., 2020. Laser powder bed fusion of AA7075 alloy: Influence of process parameters on porosity and hot cracking, Additive Manufacturing 35, 101270.

[8] Liu, Z., Zhang, D., Sing, S., 2014. Interfacial characterization of SLM parts in multimaterial processing: Metallurgical diffusion between 316L stainless steel and C18400 copper alloy, Materials Characterization 94, p. 116.

[9] Gong, M., Meng, Y., Zhang, S., Zhang, Y., Zeng, X., Gao, M., 2020. Laser-arc hybrid additive manufacturing of stainless steel with beam oscillation, Additive Manufacturing 33, 101180.

[10] Wu, D., Liu, D., Niu, F., Miao, Q., Zhao, K., Tang, B., Bi, G., Ma, G., 2020. Al–Cu alloy fabricated by novel laser-tungsten inert gas hybrid additive manufacturing, Additive Manufacturing 32, 100954.

[11] Liu, D., Wu, D., Ma, G., Zhong, C., Niu, F., Gasser, A., Schleifenbaum, J., Bi, G., 2020. Effect of post-deposition heat treatment on laser-TIG hybrid additive manufactured Al-Cu alloy, Virtual and Physical Prototyping 15, p. 445.

[12] Peng, J., Liu, Y., Sun, Q., 2021. Evolution of crystallographic orientation, columnar to equiaxed transformation and mechanical properties realized by adding TiC_{ps} in wire and arc additive manufacturing 2219 aluminum alloy, Additive Manufacturing 39, 101878.

[13] Park, J.Y., Lee, J.S., Choi, B.K., Hong, B.G., Jeong, Y.H., 2008. Effect of cooling rate on mechanical properties of aged ITER-grade Cu-Cr-Zr, Fusion Engineering and Design 83, p. 1503.

[14] Dong, B., Cai, X., Lin, S., Li, X., Fan, C., Yang, C., Sun, H., 2020. Wire arc additive manufacturing of Al-Zn-Mg-Cu alloy: Microstructures and mechanical properties, Additive Manufacture 36, 101447.

[15] Li, J., Chang, L., Li, S., 2018. Microstructure and properties of as-cast Cu-Cr-Zr alloys with lanthanum addition, Journal of Rare Earths 36, p. 424.

[16] Popovich, A., Sufiiarov, V., Polozov, I., Borisov, E., Masaylo, D., Orlov, A., 2016. Microstructure and mechanical properties of additive manufactured copper alloy. Materials Letters 179, p. 38.